

ESD-TR-67-325
ESTI FILE COPY

ESD-TR-67-325

ESD RECORD COPY
RETURN TO
SCIENTIFIC & TECHNICAL INFORMATION DIVISION
(ESTI), BUILDING 1211

ESD ACCESSION LIST

ESTI Call No. AL 57549

Copy No. / of / cys.

Semiannual Technical Summary

Seismic Discrimination

30 June 1967

Prepared for the Advanced Research Projects Agency
under Electronic Systems Division Contract AF 19(628)-5167 by

Lincoln Laboratory

MASSACHUSETTS INSTITUTE OF TECHNOLOGY

Lexington, Massachusetts



AD0657327

The work reported in this document was performed at Lincoln Laboratory, a center for research operated by Massachusetts Institute of Technology. This research is a part of Project Vela Uniform, which is sponsored by the U.S. Advanced Research Projects Agency of the Department of Defense; it is supported by ARPA under Air Force Contract AF 19(628)-5167 (ARPA Order 512).

This report may be reproduced to satisfy needs of U.S. Government agencies.

This document has been approved for public release and sale; its distribution is unlimited.

Non-Lincoln Recipients

PLEASE DO NOT RETURN

Permission is given to destroy this document
when it is no longer needed.

MASSACHUSETTS INSTITUTE OF TECHNOLOGY
LINCOLN LABORATORY

SEISMIC DISCRIMINATION

SEMIANNUAL TECHNICAL SUMMARY REPORT
TO THE
ADVANCED RESEARCH PROJECTS AGENCY

1 JANUARY - 30 JUNE 1967

ISSUED 25 JULY 1967

LEXINGTON

MASSACHUSETTS

ABSTRACT

In continuation of work on networks embodying both large and small arrays, plans have been prepared for a second Large Aperture Seismic Array (LASA) station. Studies of on-line detection and location and also signal-to-noise improvement using large array structures are continuing. Significant progress in the discrimination area using relative excitation of body and surface waves is reported.

Accepted for the Air Force
Franklin C. Hudson
Chief, Lincoln Laboratory Office

SUMMARY

This is the seventh Semiannual Technical Summary Report on Lincoln Laboratory's work for the Advanced Research Projects Agency on the seismic discrimination problem (Vela Uniform).

During this reporting period, considerable attention was given to preparations for a possible second large array station, hopefully to be located in Norway. A tentative rough system design was worked out, based on Montana experience, and a seismic survey of the area was planned which will provide suitable corrections to the initial design (Sec. VI). Analytical studies of seismic networks embodying several large arrays are continuing (Sec. I).

In the area of discrimination techniques (Sec. II), the principal new result involves studies of body- and surface-wave magnitude differential. On a large number of blasts and earthquakes, complete separation occurred. Currently, this discriminant is usable down to body-wave magnitude 4.7 for Central Asia; below this level, surface waves are not detectable in Montana.

In Sec. III, developments in the on-line detection and location of events in large array structures are discussed; off-line array processing results of both long- and short-period signals are presented in Sec. IV.

Section V summarizes recent activities at the Montana LASA by Lincoln and its subcontractor, particularly automatic monitoring and fault analysis experiments.

P. E. Green

CONTENTS

Abstract	iii
Summary	v
Glossary	viii
I. SEISMIC SURVEILLANCE NETWORKS	1
A. Network Simulations	1
B. Surface-Wave Detection Study	2
II. IDENTIFICATION	3
A. Surface- vs Body-Wave Magnitude Results	3
B. Reference Population of Events	3
C. Ratios of Spectral Densities	5
D. Phase Identification Using Beam-Power Displays	7
III. LASA DETECTION AND LOCATION	11
A. Automatic Station Bulletin	11
B. Observations in Honshu Area	12
C. Kurile Observations	12
D. Location by Beamsplitting	13
IV. ARRAY PROCESSING	15
A. Summary of Short-Period Results	15
B. Summary of Long-Period Results	17
C. Adaptive Array Processing	19
D. Matched Filtering of Long-Period Rayleigh Waves	21
E. Patterns	23
V. MONTANA LASA SYSTEM	27
A. Automatic Monitoring and Fault Analysis	27
B. LDC Analog Signal Distribution	27
C. Summary of System Modifications and Tests Performed by Phileo Corporation	28
VI. SECOND LASA	31
A. Norwegian Noise Survey	31
B. Seismic System Studies	32

GLOSSARY

AFOSR	Air Force Office of Scientific Research
AFTAC	Air Force Technical Applications Center
ARPA	Advanced Research Projects Agency
BED	Beamformer-Event Detector
ERI	Earthquake Research Institute (University of Tokyo)
FASTABUL	Fast Automatic STATION BULLETIN
LASA	Large Aperture Seismic Array
LDC	LASA Data Center
PLINS	Phone Line Interface System
SATSR	Semiannual Technical Summary Report
SEM	Subarray Electronics Module
SNR	Signal-to-Noise Ratio
TFO	Tonto Forest Observatory
USCGS	United States Coast and Geodetic Survey

SEISMIC DISCRIMINATION

I. SEISMIC SURVEILLANCE NETWORKS

In addition to our studies of the ability of large arrays to make the measurements necessary for the application of various discrimination techniques, we are attempting to simulate the overall performance of world-wide networks, containing one or more large arrays, with respect to detection and discrimination. One feature of these studies is their sensitivity to different ways of modeling the arrays themselves; another feature is the net effectiveness of arrays compared with conventional stations.

Two such simulations are now in progress, treating two discriminants independently. In the first, we are studying the accuracy of measurement by a network of epicenter and source depth, from P-wave arrival times only (see Sec. I-A below). In the second (Sec. I-B), we are concerned with the detection of surface waves and the measurement of a surface-wave magnitude.

A. NETWORK SIMULATIONS

In the last Semiannual Technical Summary Report, we reported the initiation of a system simulation study of the determination of epicenters by an extended network of stations, some of which are large arrays. We mentioned that there were several ways of characterizing an array as an element in such a network, and three of these have been studied and compared. In the first, the array (containing N elements) is modeled as N separate, conventional stations; in the second, the array is treated as a single station capable of reporting arrival times with an accuracy better than a conventional station by the factor \sqrt{N} . A third method, intended to interpolate between the others, represented the array as a collection of M stations ($M < N$), which is credited with a $\sqrt{N/M}$ improvement factor in accuracy. The three models are similar, in terms of the actual simulation program, but not identical. However, no significant difference in network performance was found for these models.

In order to assess the usefulness of large arrays as network elements, we computed the coverage resulting from a 13-element network of conventional stations and then the coverage for two series of improvements to this network: one by adding up to 3 large arrays, and another by adding up to 12 more conventional stations. In each case, the event magnitude required for 500-km² epicenter accuracy was computed on a grid of points in the northern hemisphere, and the average magnitude over this hemisphere was used as a measure of coverage. In all cases, the actual magnitudes varied sufficiently little over the hemisphere to make this simple comparison meaningful. The results showed the expected diminishing rate of improvement with the continued addition of either type of station, but the large arrays were sufficiently superior so that the results obtained by adding three arrays were roughly the same as those obtained by adding 12 conventional stations. Of course, the results will depend upon the particular geometries employed, but further studies comparing detailed performance for events in Asia or Eastern Europe have confirmed that, on our model, one or two large arrays can provide as much improvement in performance of a given network as the addition of 10 or 12 conventional arrays.

Section I

The system simulation has been extended so that source depth is now estimated, which has the corollary effect that four or more station detections are required now for network detection. We found that, for reasonable network geometries, an epicenter accuracy of 500 km^2 was consistent with a theoretical depth error of the order of 10 km. The study was then modified so that the event magnitude which is computed is the magnitude required to produce an epicentral error no larger than 500 km^2 and, at the same time, a depth error no larger than 15 km. Some coverage patterns have been computed in this way, but as yet not enough to determine whether or not this method of analysis will lead to any significant change in the relative effectiveness of arrays and conventional stations.

These studies, of course, are subject to the criticism that only the random component of the arrival-time errors is accounted for. As mentioned in the previous report,[†] it is assumed that station corrections and travel-time anomalies are well enough known to remove all biases. This assumption is probably fair for all but the source-dependent part of the travel-time anomalies of aseismic regions, and studies are continuing in an attempt to evaluate the effect of such biases on network performance.

The results obtained to date will be described in a report now in preparation.

B. SURFACE-WAVE DETECTION STUDY

A system simulation study of the ability of a seismic network to detect surface waves has been initiated. It is assumed that body waves have already been detected, and the entire system is said to have detected surface waves (and determined a surface-wave magnitude) if one or more of its stations detects these waves. We assume that all stations are capable of matched-filter processing (see Sec. IV-D) and that array stations have an additional gain of a factor of $N^{1/2}$, where N is the number of array elements. Using noise levels and matched-filter processing gains based on LASA data, we find that surface waves should be detectable down to a surface-wave magnitude of about 2.0 over large areas of the world, with a network containing on the order of 20 conventional stations. [For shallow-focus earthquakes, a surface-wave magnitude of 2.0 is equivalent to a body-wave magnitude of 3.8 (see Sec. II-A).] Moreover, each large array is equivalent to several conventional stations in its contribution to overall network performance.

E. J. Kelly

[†]Semiannual Technical Summary Report to the Advanced Research Projects Agency on Seismic Discrimination, Lincoln Laboratory, M.I.T. (31 December 1966), DDC 646677.

II. IDENTIFICATION

A. SURFACE- VS BODY-WAVE MAGNITUDE RESULTS

A useful discriminant for distinguishing between natural seismic events and underground nuclear explosions is based on the relationship between the surface- and body-wave magnitudes. Theoretical calculations due to Keilis-Borok¹ have shown that the most efficient excitation of surface waves occurs at wavelengths approximately four times the dimension of the source, that is, the source region acts as a quarter-wavelength antenna. The source dimensions for an underground nuclear explosion are usually much smaller than those of an earthquake of comparable body-wave magnitude. Thus, we would expect the earthquakes to excite the longer periods of surface waves more efficiently than the underground nuclear explosions. This conclusion has been verified experimentally by several previous investigators.^{2,3}

An experiment is being performed using LASA data to determine how effective a single LASA is in using this discriminant teleseismically. The body- and surface-wave magnitudes for events from the Central Asian area have been computed. The weaker events have been subjected to both maximum-likelihood and delay-and-sum processing, which achieve about 14 and 11 db of signal-to-noise ratio (SNR) enhancement, respectively. In addition, if required, matched filtering (described in Sec. IV-D) can be used to achieve another 6 to 10 db of SNR enhancement.

The body-wave magnitude m_b is based on the amplitude of short-period waves recorded at teleseismic distances and is computed according to the formula given by Gutenberg and Richter⁴

$$m_b = \log w/T + Q + S$$

where w is the maximum zero-to-peak ground amplitude (in millimicrons) of the first three to four cycles of the P-wave recorded on vertical-component short-period seismometers, T is the period (in seconds) of the observed short-period cycle, Q is a parameter which depends on epicentral distance and focal depth and is tabulated in Fig. 5 of a paper by Gutenberg and Richter,⁴ and S is a ground correction representing average station ground conditions which for convenience is taken to be zero in the case of the LASA.

The surface-wave magnitude M_s is based on the amplitude of Rayleigh waves with periods of about 20 sec and is used as a measure of the excitation of the long-period waves. The surface-wave magnitude is computed as

$$M_s = \log A - \log B + C + D$$

where A is the ground amplitude of Rayleigh waves (in millimicrons) with periods of about 20 sec recorded on vertical-component long-period seismometers, $-\log B$ is a parameter which depends on epicentral distance and is tabulated in Table 4 of a paper by Gutenberg,⁵ and $C + D$ is a correction for station, depth, and radiation pattern, and is (for convenience) taken to be zero. An empirical relationship between M_s and m_b has been formulated by Gutenberg and Richter,⁴

$$M_s = 1.59 m_b - 3.97$$

This equation relates the amplitudes of surface waves to those of body waves for earthquakes and was determined from a large body of data for earthquakes of body-wave magnitude greater than 6.0.

Section II

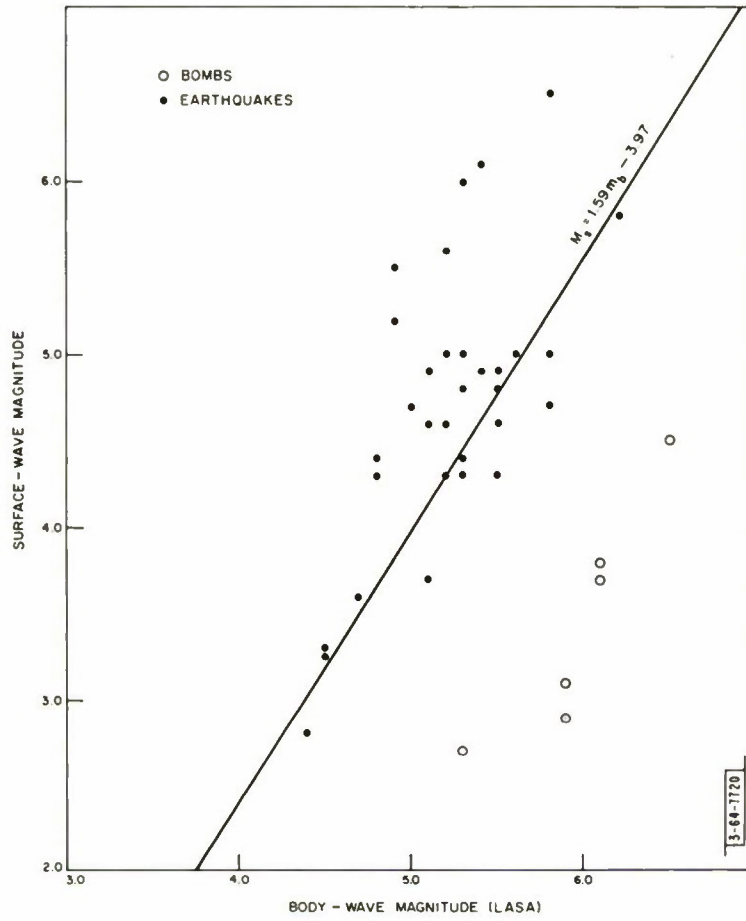


Fig. 1. LASA surface- vs body-wave magnitudes for Central Asian events.

The results of the experiment are given in Fig. 1, which shows the M_s vs m_b for the Central Asian events, as well as the Gutenberg-Richter empirical relationship. It is seen from Fig. 1 that the preliminary results are very encouraging since there is a perfect separation between the earthquake and bomb populations. It is also encouraging to note that the body-wave detection threshold for the earthquakes, for LASA operation at teleseismic distances, is approximately 4.4. The threshold for the bombs is approximately a body-wave magnitude of 5.3.

The body-wave magnitude shown in Fig. 1 was obtained by averaging over several widely separated sensors at LASA, so that a relatively good determination of body-wave magnitude is obtained, compared with what would be obtained at a single conventional type station. It should be mentioned that the surface-wave magnitude data given in Fig. 1 were also plotted vs the U. S. Coast and Geodetic Survey (USCGS) body-wave magnitude. Although the scatter of the data was diminished by doing this, the separation of the earthquake and explosion populations was somewhat better using LASA, rather than CGS, body-wave magnitude.

Preliminary indications obtained from events from the Kurile-Kamchatka region show that other regions give rise to earthquakes for which the M_s vs m_b characteristic may be quite different from that of the Central Asian area. In fact, the separation between the earthquake and explosion populations may be worse for these regions than that found for the Central Asian region. This has indeed been found to be the case in a study of Aleutian earthquakes.⁶

J. Capong
R. J. Greenfield
R. T. Lacoss

B. REFERENCE POPULATION OF EVENTS

All Sino-Soviet events from the November-December 1966 recording observations and all recorded Sino-Soviet events for which pP was not observed on LASA data from December 1966 to the end of April 1967, along with some earlier explosion data, are being used as a reference population to determine statistics on the performance of the complexity, spectral ratio, and body- to surface-wave magnitude as discriminants to separate explosive and natural events. Approximately 195 events are included in the list, ranging in magnitude from 3.7 to 6.5. Each event is being processed by standard programs to produce a set of long-period and a set of short-period beams which will be used for analysis of each event.

H. W. Briscoe

C. RATIOS OF SPECTRAL DENSITIES

A study of the use for discrimination of ratios of spectral densities of the same phase at two frequencies indicates that there is a difference between the spectra of explosive and natural sources that can be detected at teleseismic distances (see Sec. II-B of SATSR for 31 December 1966, DDC 646677). Figure 2 shows the measured short-period P-wave spectral ratio of a number of explosions and earthquakes, as a function of magnitude.

The major limitation on the use of the spectral ratio seems to be signal-to-noise level, particularly at the low-frequency end of the short-period spectrum (0.3 Hz). The apparent importance of this region of the spectrum is indicated by Fig. 3 which shows the difference in the average spectra of a small sample of earthquakes and that of a small sample of explosions.

Section II

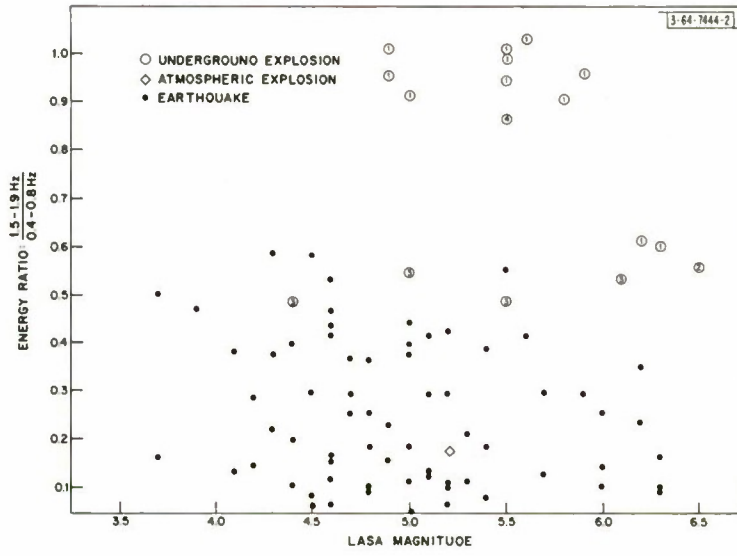


Fig. 2. Measured ratio of P-energy of two frequencies for blasts and earthquakes. Circles refer to different test sites.

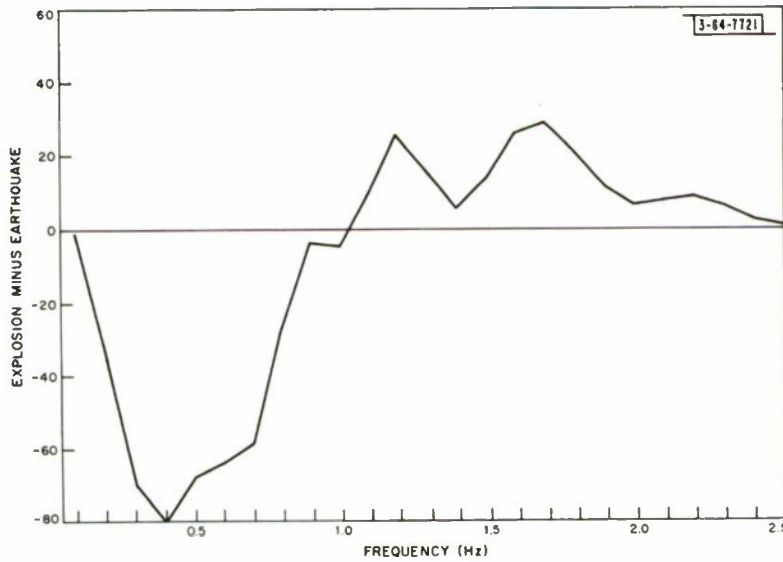


Fig. 3. Difference between average amplitude spectral density for several earthquakes and explosions as a function of frequency. (Magnitude 5.5 to 6.5.)

Although more events from a wider range of magnitudes are being used in continuation of this study, the preliminary result shows a distinct difference in the 0.3- to 0.7-Hz range of frequencies.

One technique that should improve the measurement for the "spectral ratio" discriminant is to determine the noise spectrum using a sample of noise preceding the signal and subtract the noise spectrum from the signal spectrum. Assuming stationary noise, this procedure should have two advantages: (1) for low signal-to-noise levels, the spectral ratio measurement is more accurate, and (2) there is a clear indication when the signal level is less than the variation in the noise and the measurement is meaningless. By applying this technique to delay-and-sum beam data using the subarray sums from LASA, the SNR became too low for reliable spectral ratio measurement using the apparent optimum frequency ranges at magnitudes between 4.5 and 5.0. Above magnitude 5.0, the separation improved slightly.

Since the noise in the low-frequency band has been shown to be coherent across a subarray, optimum processing procedures such as maximum-likelihood processing should result in a significant improvement in signal-to-noise level compared with beamforming. In order to test this hypothesis, a large earthquake was processed using maximum likelihood and beamforming, and the spectra compared. Since there was a good SNR on single sensors for this event, the spectra of the processed data should be similar to each other and to the spectrum of a raw trace at low frequencies. (Amplifier distortion on a large event may cause disagreement at 1.5 Hz and above.) Figure 4 shows the spectra of the maximum-likelihood trace, the beam, and a single sensor. It can be seen that at low frequencies the signal on the maximum-likelihood processed trace seems to have been partly suppressed. The signal suppression at low frequencies is probably due to the fact that the seismometers in the array are calibrated and equalized at 1 Hz, but may have significant variations in their characteristics at low frequencies so that the basic assumption of identical signal at all sensors would be invalid. Attempts are being made to rerun the experiment with the raw traces equalized in the low-frequency band.

H. W. Briscoe
R. Walsh

D. PHASE IDENTIFICATION USING BEAM-POWER DISPLAYS

In a previous report,⁷ an unsuccessful experiment was described whose intent was to improve P and pP visibility by plotting, as a function of time, the ratio of power in a beam pointed at P (and pP) to the power from all other directions. It was concluded that a side-by-side display of power vs time in a number of adjacent beams might be more revealing. Such a display has now been implemented and a few tests made.

Figure 5(a-c) shows a typical use of such beam-power displays. In Figs. 5(a) and (c), power from each of 32 beams is plotted in the form of trace intensity as a function of time.† Figure 5(b) shows the locations of the various beams on a map of the world as a function of the polar coordinates azimuth and wave number. Smoothing time is 2.0 sec, and total duration of each display is 160 sec. At the top of each display is a series of dots giving, as a function of beam number,

† This form of display of power vs time for a set of 32 inputs was originally developed for the case where the 32 variables were the outputs of adjacent filter bands, thus forming a "sonogram" as described in Sec. III of the SATSR for 30 June 1964, DDC 443444.

Section II

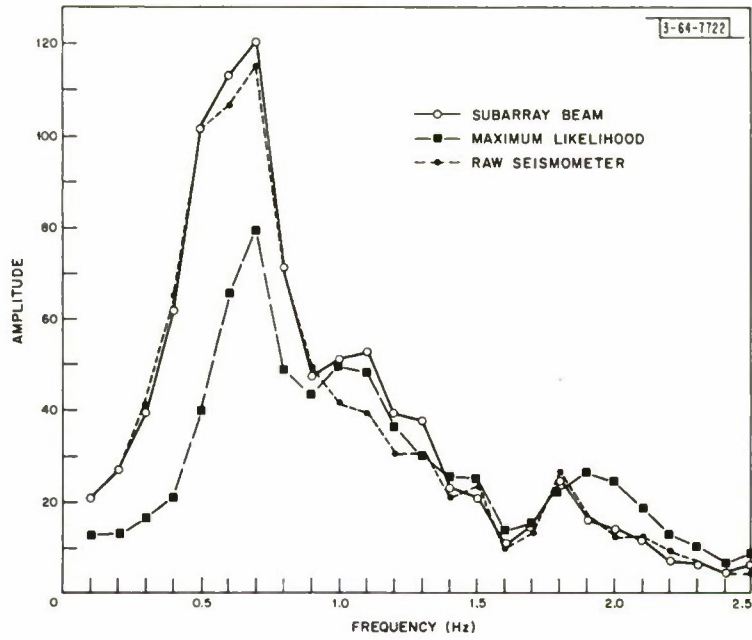


Fig. 4. Amplitude spectra of raw and processed seismometer data from an earthquake in the Aleutian Islands.



(a) (b) (c)
 Fig. 5. Displays of beam power as function of time. (a) Azimuth fixed, wavenumber varied; (b) map of world in wavenumber and azimuth (P-phase, 1.0 Hz); (c) wavenumber fixed, azimuth varied. (Dec. 22, 1966, 17:26 Z, Kuriles, $m(CG5) = 4.7$, $h(CG5) = 38$ km.)

Section II

the energy measured over the interval between the two adjustable cursor lines on the display below. The arrow heads point to the location, in time and beam number, at which various phases arrive. The phase arriving at the expected time of PcP was originally designated as such until the beam display of Fig. 5(a) revealed that it did not concentrate at the wave number expected for PcP, but instead had the same wave number as P, and therefore was possibly pP for a source depth of 120 km. This assumption is corroborated by the presence of a later phase which fits the sP time for 120 km. The phases marked "?" remain unidentified, but it is clear that the first of these is not the best candidate for pP as was originally assumed from the raw traces.

This form of display appears to be quite helpful in identifying secondary body-wave phases and in disentangling simultaneously arriving events. Experiments on a number of events at various depths are continuing.

P. E. Green
A. P. Tripp

REFERENCES

1. V. I. Keilis-Barak, "Differences in the Spectra of Surface Waves from Earthquakes and from Explosions," Tr. Inst. Fiz. Zemli 182, Na. 15, 88 (1961).
2. F. Press, G. Dewort, and R. Gilman, "A Study of Diagnostic Techniques for Identifying Earthquakes," J. Geophys. Res. 68, 2909 (1963).
3. J. N. Brune, A. Espinosa, and J. Oliver, "Relative Excitation of Surface Waves by Earthquakes and Underground Explosions in the California-Nevada Region," J. Geophys. Res. 68, 3501 (1963).
4. B. Gutenberg and C. F. Richter, "Magnitude and Energy of Earthquakes," Ann. Geophys. 9, 1 (1956).
5. B. Gutenberg, "Amplitudes of Surface Waves and Magnitudes of Shallow Earthquakes," Bull. Seismol. Soc. Am. 35, 3 (1945).
6. R. C. Liebermann, C. Y. King, J. N. Brune, and P. W. Pomeroy, "Excitation of Surface Waves by the Underground Nuclear Explosion of Long Shot," J. Geophys. Res. 71, 4333 (1966).
7. Semiannual Technical Summary Report to the Advanced Research Projects Agency on Seismic Discrimination, Sec. II-H, Lincoln Laboratory, M. I. T. (30 June 1965), DDC 467395.

III. LASA DETECTION AND LOCATION

A. AUTOMATIC STATION BULLETIN

Two versions of a fast automatic station bulletin program (FASTABUL and NOTCHSTABUL) were described in Sec. III-B of the last Semiannual Technical Summary Report (31 December 1966, DDC 646677). The NOTCHSTABUL program has now been in use at LASA for several months, and it was noticed that the major shortcoming was in the picking of the P-phase onset. Often the program would pick the "up" part of the waveform on some subarrays and the "down" part on others. In its culling process, only a consistent set would be used, viz., the majority. As long as the outermost subarrays were included, the epicenter calculation would be good because of the large base line, but in a large number of cases some (or all) of the outermost subarrays would be in the minority set. The smaller base line would determine locations with less precision.

A new version of the program (called CROSSTABUL) corrects this defect by determining relative arrival times by cross correlation, and further improves the program by preprocessing the input waveforms to enhance the SNR. Since CROSSTABUL generates self-consistent and more accurate time and amplitude picks for all 24 traces, it can perform several extra tasks:

- (1) A delay-and-sum beam pointed to the source is automatically generated.
- (2) Two minutes of this beam output, along with the 24 processed traces, are edited and stacked on a library tape in a standard format. One library tape has a capacity of about 100 events. Thus, if CROSSTABUL is run on every teleseism flagged by the TSD, a selected portion of every such event can be saved with a considerable saving of magnetic tape.
- (3) The time picks determined by CROSSTABUL are sufficiently accurate that the main sources of error are the simple station corrections used by FASTABUL which are functions of one variable (azimuth). Station corrections (i.e., the time residuals from the best fitting plane wave) are automatically generated and saved by CROSSTABUL. They can be used to update a table of travel time anomalies as a function of epicenter location. A threshold is used to allow only clean events (with presumably accurate time picks) to update this table. When sufficient data have accumulated, two-dimensional station corrections (i.e., functions of azimuth and distance) can be incorporated which should improve the usefulness and accuracy of the program. These station corrections will be self-consistent in the sense that they will be applied in the same manner in which they were measured. As more and more entries are made to this table, a new set of station corrections will be automatically generated and used in the first part of the program. Thus, the program will "teach itself" using a self-consistent measuring method.
- (4) The amplitude residuals (i.e., the amplitude anomalies from the average amplitude) will be saved and used to keep updating a table of amplitude scatter vs azimuth and distance.
- (5) The amplitude, period, magnitude, complexity, and first motion calculations are improved by using the beam waveform instead of averaging 24 individual measurements, any of which is more likely to be contaminated by microseismic noise. This should decrease the variance in the above measurements.

CROSSTABUL is not a real-time program in the sense that FASTABUL was. However, it can be an on-line program if it can complete all its operations before another event occurs.

Section III

The maximum CROSSTABUL processing time using the PDP-7 machine is 15 min. per event, giving an on-line data rate of about 100 events per day. The use of FASTABUL at the Montana LASA Data Center to prepare the daily station bulletin never took advantage of its real-time capabilities; it was used off-line on the spare PDP-7 computer, taking about 10 min. per event. Consequently, it has been felt that this more powerful processing procedure would be an improvement.

The CROSSTABUL program has been tested using the same 70 events that were used to check the performance of FASTABUL and NOTCHSTABUL. The results using this family of events show that CROSSTABUL is far superior in locating events and finding their origin time — the rms error is about halved. The estimates of the period and first motion are much more reliable due to the fact that they are determined from the beam which shows an improved SNR. The magnitude (and amplitude) estimates are significantly lower than the CGS figures because they are computed from the beam which shows some signal loss and because of the increased SNR and the way amplitude is defined, i.e., the peak-to-peak difference of the first two detectable cycles.

NOTCHSTABUL is superior to CROSSTABUL when the signal amplitude is less than 1 or 2 μ . Because of this, and the more complicated operating procedure, CROSSTABUL is not being used at the LASA Data Center.

P. L. Fleck

B. OBSERVATIONS IN HONSHU AREA

The analysis described in the last Semiannual Technical Summary Report has been completed for all events for which LASA taps are available. The results of this experiment will be described in a Technical Note now in preparation.

R. M. Sheppard

C. KURILE OBSERVATIONS

The data collected at LASA during November and December 1966, when ocean-bottom seismometers were in place off the Kurile Islands, are being used in two separate experiments. First, data collected from events from the entire Sino-Soviet area are being used to form a reference population, as described in Sec. II-B of this report. In the second effort, data from LASA are being compared with data on the shot locations and ocean-bottom seismometer data to provide a better understanding of LASA capabilities.

LASA magnitudes have now been measured for all shots either seen by LASA or recorded for off-line analysis. The magnitudes are listed below. For questionable detections or shots not detected (denoted by *), an upper bound for the magnitude has been determined by computing the magnitude of the largest burst of noise (or signal) occurring on filtered beams at the expected arrival time.

<u>Date</u>	<u>Shot Time</u>	<u>LASA Magnitude</u>
11/08/66	06:53:02	3.6
11/09/66	23:23:03	4.2
11/10/66	06:25:04	<3.6*
11/12/66	23:31:03	<3.6*
11/13/66	05:48:03	<3.6*
12/02/66	22:30:02	3.6
12/03/66	05:21:03	4.0
12/03/66	22:49:03	4.4
12/04/66	22:24:03	3.9
12/05/66	03:21:03	<3.5*

Although only preliminary time picks from the ocean-bottom seismometers have been provided so far, a comparison with LASA data indicates that most events seen at more than three ocean-bottom seismometers were detectable on LASA data.

H. W. Briscoe

D. LOCATION BY BEAMSPLITTING

LASA on-line detection and location, which currently uses "triangulation" from a number of individual subarray outputs (and employs programs such as FASTABUL, NOTCHSTABUL, and CROSSTABUL), is ultimately to be changed so that multiple beams are used. Each beam output has the full array SNR gain.

To check the feasibility of this approach, a beamsplitting program has been written which forms a square array (21×21) of beams uniformly separated by 0.5° increments in latitude and longitude, thus covering an area of $10^\circ \times 10^\circ$. The center of the array can be aimed at any point in the teleseismic coverage region from LASA. Each of the beams has an independent event detector[†] followed by an integrator which measures the energy in each beam for 5 sec starting at the event detector trigger time. The outputs, measured in decibels down from the maximum, appear on a two-dimensional contour plot.

An example of the output from one event is shown in Fig.6. The program can be used to (1) determine the precision and accuracy with which an event can be located by beamsplitting (in this large-magnitude example, a small fraction of a degree), (2) determine real beam patterns and sidelobes, and (3) investigate how energy in each beam varies with time as seismic waves from an actual event or events arrive at the array.

P. L. Fleck

[†]H. W. Briscoe and P. L. Fleck, "A Real-Time Computing System for LASA," Proc. Spring Joint Computer Conference, Boston, Massachusetts, 26 - 28 April 1966, DDC 642202.

Section III

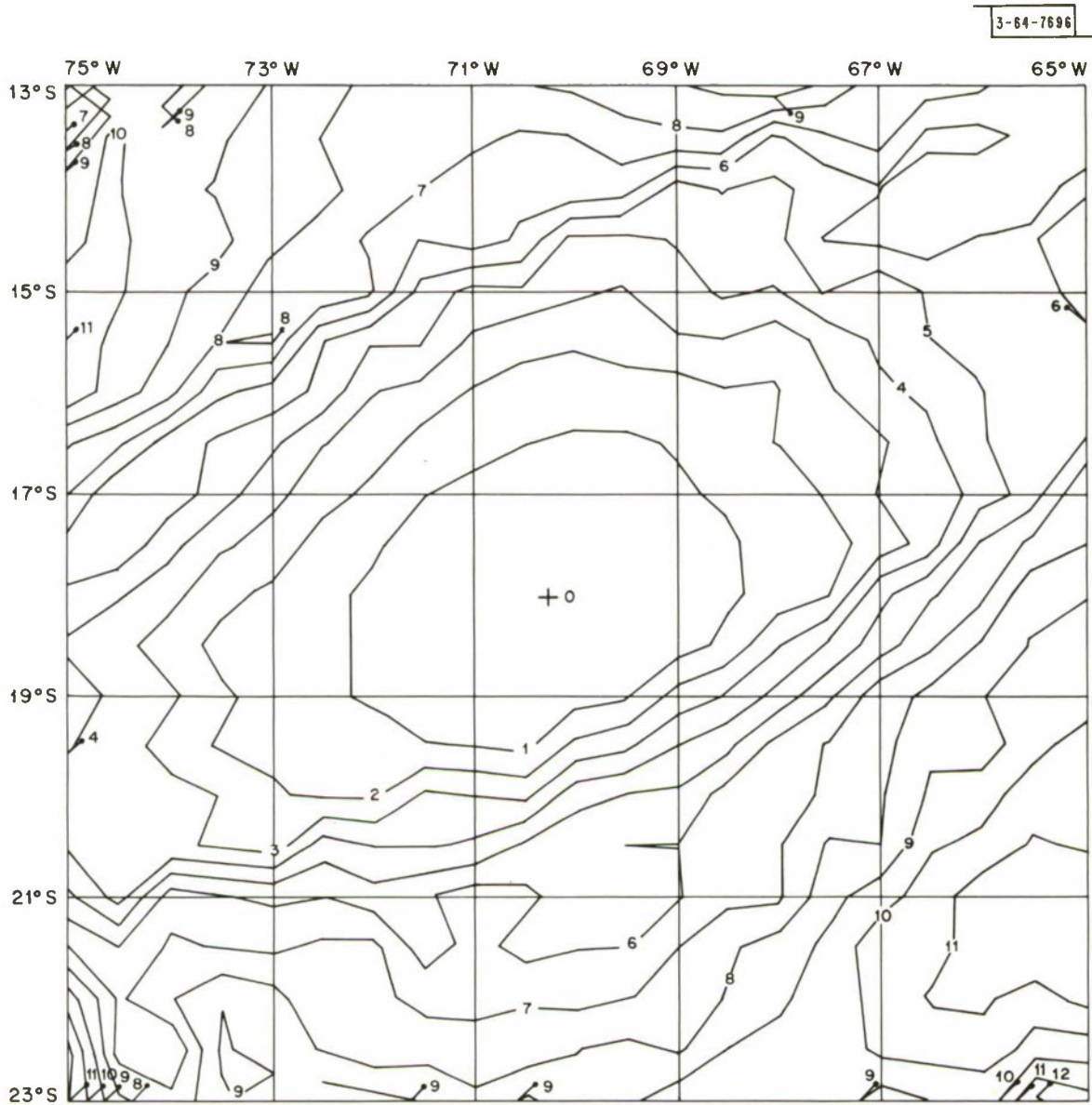


Fig. 6. Beam pattern from on event of 12 January 1967. Latitude 18°S, longitude 70.3°W. Circle shows beamsplit maximum; cross shows CGS location.

IV. ARRAY PROCESSING

A. SUMMARY OF SHORT-PERIOD RESULTS

An attempt was made to combine the LASA results on SNR gain of maximum likelihood, i.e., filter-and-sum (FS) processing, and delay-and-sum (DS) processing (that is, beamforming), for various apertures and frequencies, to serve as a guide in the design of future LASA subarrays. The FS processing results were obtained using LASA data that were bandpass prefiltered, 0.6 to 2.0 Hz, with a three-pole Butterworth filter. The beamforming results were obtained using LASA data that were prefiltered with narrow-band filters of bandwidth 0.1 Hz and center frequencies of 0.6, 1.0, and 1.5 Hz.

The results are presented in Fig. 7 which shows the SNR gain of DS and FS processing relative to the gain which would be obtained for independent noise, namely $10 \log_{10} N$ (where N is the number of sensors), vs the element density. These results indicate that if the DS gain is to be within 1 db of this norm at 1.0 and 1.5 Hz, then the average sensor separation should be greater than about 3 km if DS processing is to be used. It is important to stress that sensors should not be placed any closer than 3 km, since this will have the effect of actually lowering the gain obtained with DS processing due to the introduction of coherent noise.

The results of Fig. 7 also show that for separations greater than about 1.6 km, the FS gain in the 0.6- to 2.0-Hz band is about 2 db better than the DS gain at 0.6 Hz, 0.5 db worse than the DS gain at 1.0 Hz, and about 2 db worse than the DS gain at 1.5 Hz. Since most of the noise power is concentrated at 0.6 Hz, when only the 0.6- to 2.0-Hz band is considered, it follows that the overall gain of DS is only about 2 db worse than that of FS for average sensor separation greater than about 1.6 km.

However, as the average sensor separation decreases beyond 1.6 km, the performance of FS relative to DS processing improves considerably. For average sensor separations less than 1.0 km, the FS gain is almost as good as or better than that of DS at 0.6, 1.0, and 1.5 Hz, and the overall gain of FS is about 5 db better than that of DS. It is important to note that the overall gain of FS for the small sensor separations is about the same as that of DS for large sensor separations.

The conclusion is that if closely spaced seismometers are used in the design of a subarray, then FS processing is required; if widely spaced seismometers are used, then approximately the same gain can be obtained with DS processing. The amount of gain to be expected for various element densities can be obtained from Fig. 7, thus facilitating the design of a subarray for a future LASA.

The signal beamforming loss vs array aperture is shown in Fig. 8. These data were obtained by simulating as well as possible an array with uniformly spaced sensors. The signal loss of DS was then measured relative to the amplitude of the average sensor. The station corrections, or time-delay corrections relative to the plane-wave approximation, were applied only to those sensors which were more than 20 km from the center of LASA. We see from Fig. 8 that a signal beamforming loss of 4.5 db is incurred for beamforming of the entire 200-km Montana LASA.

J. Capon
R. J. Greenfield
R. T. Lacoss

Section IV

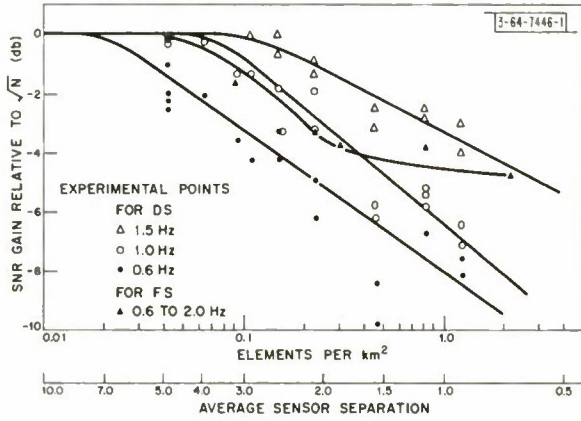
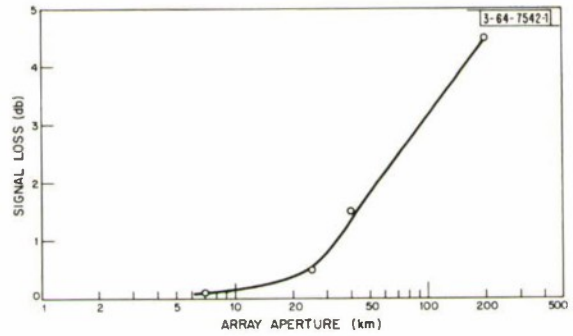


Fig. 7. Short-period SNR gain vs element density.

Fig. 8. Signal beamforming loss vs array aperture (0.6 to 2.0 Hz).



B. SUMMARY OF LONG-PERIOD RESULTS

A number of experiments were performed using data obtained from the long-period vertical array at LASA for the purpose of determining optimum long-period array configurations. The SNR gain obtained from maximum-likelihood (or FS) processing, as well as beamforming (or DS) processing, was measured as a function of aperture and number of sensors. Some preliminary tests using bandpass prefiltered data indicated that the results using prefiltered data were similar to those using unfiltered data, so that no prefiltering of the data was used in the experiments.

The experiments were performed in several ways. The gain of the entire array was measured using 21 sensors, and then, successively, it was measured as the outside and inside rings of sensors were removed from the array. Gain was also measured for an array of five sensors consisting of, successively, the A0-B, A0-C, A0-D, A0-E, A0-F rings. In addition, several results using the A0-C-D and A0-D-E rings were obtained. The data are shown in Fig. 9, which shows the SNR gain of DS and FS processing relative to the gain which would be obtained for independent noise, namely $10 \log_{10} N$ (where N is the number of sensors), vs the element density. The abscissa is also labeled in terms of average sensor separation.

These results show that if the gain relative to \sqrt{N} is to be approximately 0 db, then for DS or FS processing, respectively, element spacing should be about 15 or 45 km, respectively. However, if the gain relative to \sqrt{N} is allowed to be -1 db, then for DS processing the sensor spacing should be approximately 30 km. As a practical matter, it appears that 20- to 30-km sensor spacing for DS processing would be adequate. The use of DS instead of FS processing is desirable since DS processing is much simpler and less expensive. In addition, FS processing is much more susceptible to anomalies, such as weak sensors, than is DS processing. It should also be noted that for a given element density, FS processing has only a 3-db advantage over DS processing.

The frequency-wavenumber structure of the noise has also been determined. It was found on one noise sample that most of the noise energy lies in the 16- to 20-sec period range and that this energy is highly concentrated at a wavenumber which corresponds to an azimuth of about 25° and a velocity of 3.5 km/sec. This type of wavenumber structure is very similar to that of the long-period surface-wave signals. The steering parameters used in array processing are the azimuth of the event and a horizontal phase velocity of 3.7 km/sec, which was found to be the phase velocity of the surface waves in the 25-sec period range. Thus, if the azimuth used in array processing is the same as the azimuth of the noise source, the array processing gain should be quite low due to the similarity between the desired event and the noise. An experiment was performed to measure the gain of DS and FS processing as a function of azimuth using the A, D, and E rings at LASA. The results of this experiment are shown in Fig. 10. As expected, the gain of both DS and FS processing decreases sharply when the azimuth is in the vicinity of 25°, corresponding to the azimuth of the noise source.

One area in which FS processing has been found to be much more useful than DS processing is in the suppression of interfering long-period Rayleigh waves. The time duration of these surface waves is usually about 10 to 20 min., so that it is quite likely that an event may generate surface waves which interfere with those of a desired event. An experiment was performed to determine the effectiveness of DS and FS processing in suppressing the surface waves of an

Section IV

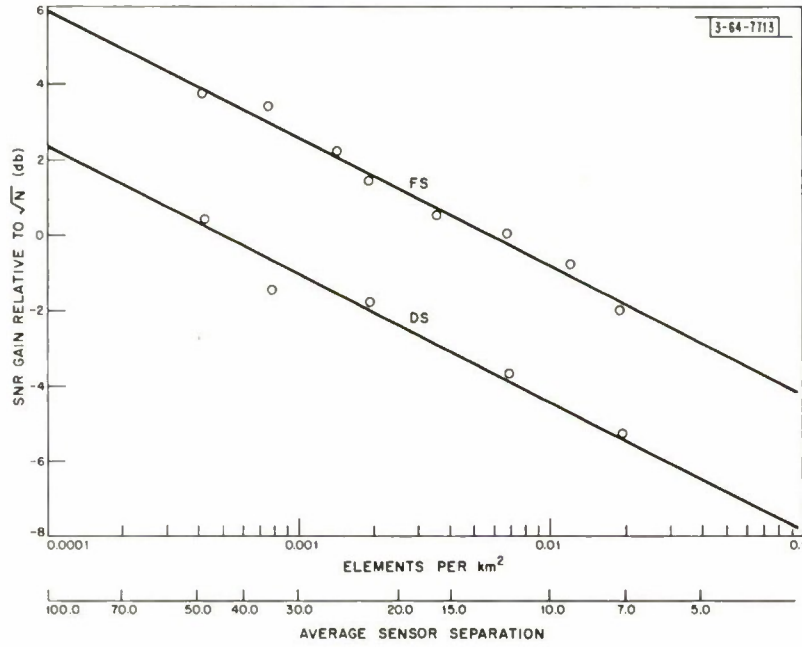


Fig. 9. Long-period SNR gain vs element density.

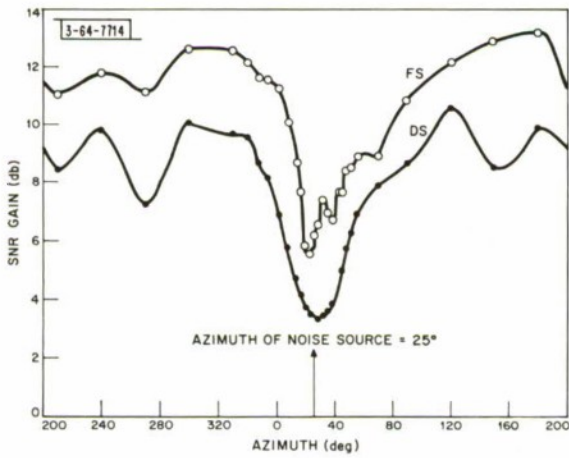


Fig. 10. FS and DS gain vs azimuth using A, D, and E rings.

interfering event while passing the surface waves of the desired event. The interfering event was taken as a 21 November 1966 Kurile Islands event,[†] and the desired event as a 12 November 1966 Argentina event.[‡] A 12 November 1966 Kurile Islands event[§] was used in the fitting interval to design the filters used in the FS processing. The surface waves of the 12 November 1966 Argentina event were hidden in the surface waves of the 21 November 1966 Kurile Islands event, by adding the traces, as indicated in Fig. 11. The results of the DS processing (shown in Fig. 11) indicate that the Argentina surface waves are not resolvable, since only 11 db of rejection of the interfering surface waves was obtained with this form of processing. However, the Argentina surface waves are visible in the FS processed trace, as this form of processing achieved about 20db of suppression of the interfering surface waves. Thus, FS processing has a clear superiority over simpler forms of processing, such as beamforming, for the purpose of rejecting interfering surface waves.

J. Capon
R. J. Greenfield
R. T. Lacoss

C. ADAPTIVE ARRAY PROCESSING

A study of adaptive array processors, mentioned under the heading "Iterative Design of Array Processors" (Sec. II-E of SATSR for 31 December 1965, DDC 630559), has been completed and a journal article is being prepared.

Two adjusting procedures were investigated in detail. The notation is as follows. Let \mathcal{P} be a $K \times K$ matrix with elements

$$\mathcal{P}_{ij} = \begin{cases} 1 - \frac{1}{K} & , \quad \text{if } i = j \\ -\frac{1}{K} & , \quad \text{otherwise} \end{cases}$$

Assume that data have been shifted in time to properly align the signals. Let $x_i(n)$ denote the output of the i^{th} seismometer at time n . The array output at time n is then

$$y(n) = \sum_{i=1}^K w_i(k) x_i(n)$$

where the $w_i(k)$ are weights resulting from the k^{th} adjustment. The vector $\underline{w}(k)$ has the $w_i(k)$ as components. The w_i must sum to unity. Let σ_i be the noise standard deviation on the i^{th} channel, and σ the average of the σ_i . Finally, define a vector

$$\hat{\underline{g}}(k) = \frac{1}{L} \sum_{j=1}^L \underline{x}(kL + j) y(kL + j)$$

and a vector $\tilde{\underline{g}}(k)$ by its components

[†] $t_o = 12:19:18$, $\Delta = 64^\circ$, $Az = 312^\circ$, h (CGS) = 40 km, m_b (LASA) = 6.0, M_s (CGS) = 5.6.

[‡] $t_o = 12:54:02$, $\Delta = 93^\circ$, $Az = 143^\circ$, m_b (LASA) = 5.0, unreported by CGS.

[§] $t_o = 12:49:58$, $\Delta = 72^\circ$, $Az = 312^\circ$, h (CGS) = 33 km, m_b (LASA) = 5.0, m_b (CGS) = 5.8.

Section IV

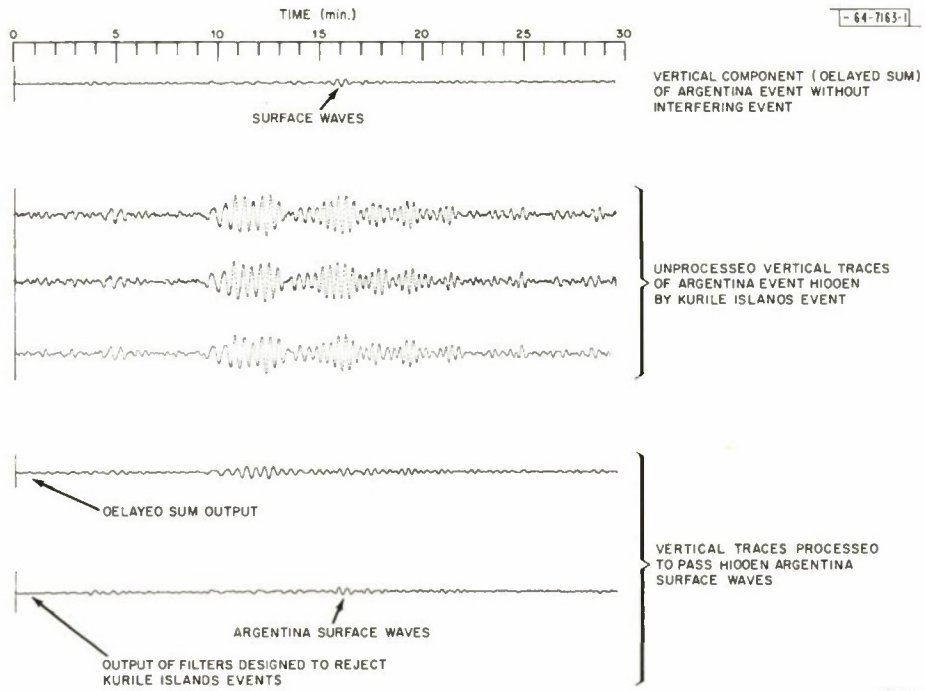


Fig. 11. Suppression of long-period interfering teleseism.

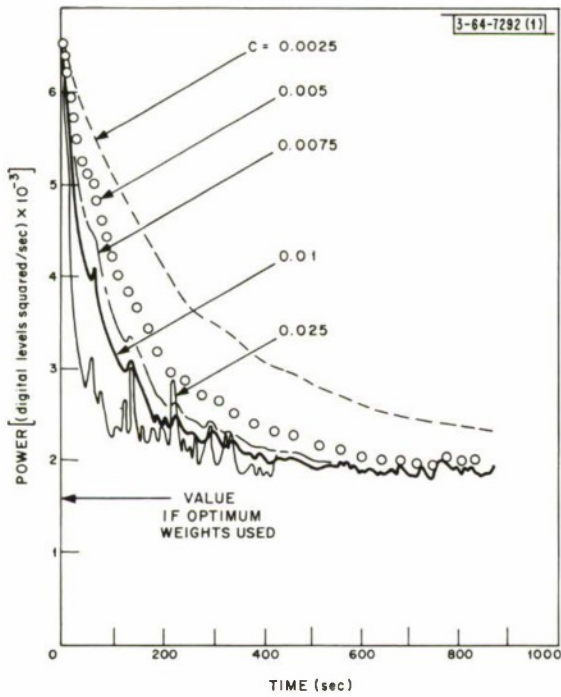


Fig. 12. Transient recovery of one-bit correlation adaptive processor.

$$\tilde{g}_i(k) = \frac{\sigma_i}{\sigma} \sin \left\{ \frac{\pi}{2L} \sum_{j=1}^L \text{sgn} [x_i(kL + j) y(kL + j)] \right\}$$

where $\text{sgn} [\dots]$ is ± 1 , depending upon the sign of the argument. L is the number of data samples between iterations. The vectors $\hat{g}(k)$ and $\tilde{g}(k)$ are both estimates of the gradient with respect to $\underline{w}(k)$ of the variance of $y(n)$.

Equations describing the two weight adjustment rules can now be written. One rule, called the clipped gradient method, is

$$\underline{w}(k+1) = \underline{w}(k) - \frac{C \mathcal{P} \hat{g}(k)}{\sqrt{\sum_{i=1}^K \hat{g}_i^2(k)}}$$

The other, the one-bit correlation method, obeys the equation

$$\underline{w}(k+1) = \underline{w}(k) - C \mathcal{P} \tilde{g}(k)$$

In both cases, C is an adjustable gain constant. Both of these adaptive laws are computationally feasible for array processing. The latter can be somewhat more efficient and requires less memory.

Figure 12 shows the recovery of the one-bit correlation adaptive law from an initial condition with all weights equal. One iteration was carried out every 25 samples, i.e., every 1.25 sec. At any time, the ordinate is the expected output noise power that the array processor would produce if weights were held constant at the value they have at that time. More data and discussion are contained in the paper.

R. T. Lacoss

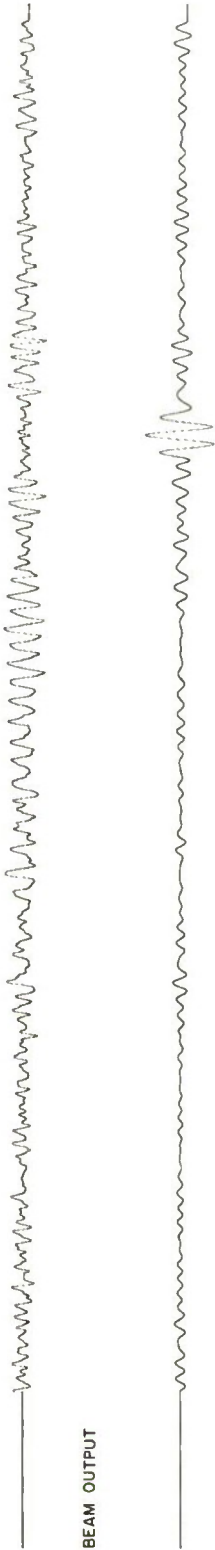
D. MATCHED FILTERING OF LONG-PERIOD RAYLEIGH WAVES

In the period range of interest, the group velocity at which Rayleigh waves propagate decreases with frequency. As a consequence of this dispersive mode of propagation, the amplitude of the Rayleigh wave train decreases with distance r from the source, at the rate $(r)^{-1/2}$. In addition to this loss due to dispersion, there are also losses due to geometric spreading of the wave, and from dissipation. Much of the loss in amplitude due to dispersion may be recovered by the use of a filter whose impulse response is matched to the Rayleigh wave train. If the noise can be assumed to be white over the signal band of approximately 0.025 to 0.050 Hz, then the matched filter is optimum in the sense that it provides the largest SNR enhancement for the long-period Rayleigh wave train.

An equivalent manner in which this optimum SNR enhancement can be obtained is to cross-correlate the received signal with a reference waveform which is a replica of the Rayleigh wave train. As is well known, the impulse response of the matched filter is a time-reversed, time-shifted version of the crosscorrelator reference waveform. It was found that a simple linear frequency-sweep reference waveform

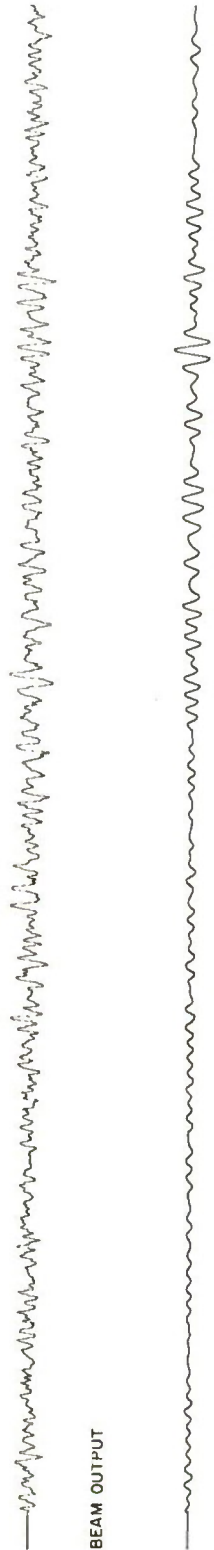
$$R(t) = \begin{cases} \sin \left[2\pi \left(f_0 + \frac{f_1 - f_0}{2L} t \right) t \right] & , \quad 0 \leq t \leq L \\ 0 & , \quad \text{otherwise} \end{cases}$$

3-64-7715



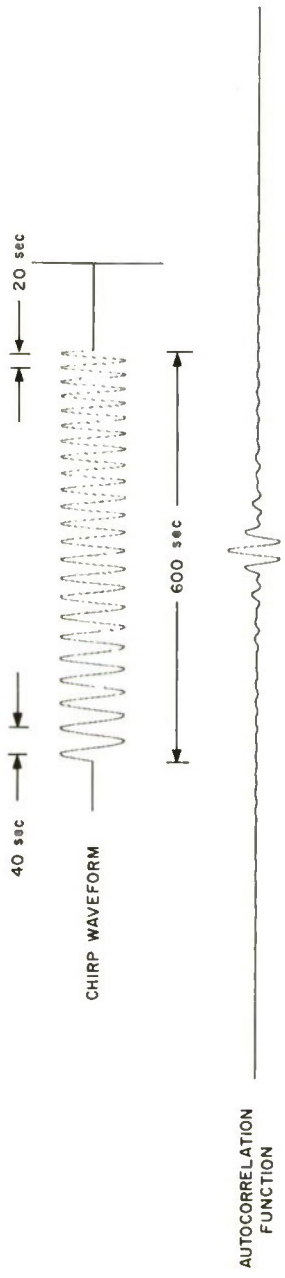
(a) STRONG EASTERN KAZAKH EVENT; $m_b = 6.1$, $M_s = 3.7$

3-64-7716



(b) WEAKER EASTERN KAZAKH EVENT; $m_b = 5.9$, $M_s = 3.1$

3-64-7717



(c) TYPICAL AUTOCORRELATION FUNCTION OF CHIRP WAVEFORM

Fig. 13. Matched filter SNR improvement for long-period Rayleigh waves.

gave satisfactory results, where f_0, f_1 are the initial and final frequencies of the dispersed Rayleigh wave train whose time duration is assumed to be L sec. This reference waveform is also known as a chirp waveform.[†] It is easily seen that the chirp waveform would be a replica of the Rayleigh wave train if the group velocity were a linear function of frequency and if the dissipation loss were uniform with frequency over the seismometer pass band.

The theoretical SNR improvement for the matched filter, assuming a perfect match between the Rayleigh wave and the impulse response of the filter, is given by the time-bandwidth product $(f_1 - f_0) L$. It is found typically that $L = 600$ sec, $f_0 = 0.025$ Hz, and $f_1 = 0.050$ Hz, so that the theoretical gain is equal to a factor of 15 or about 12 db. In practice, it is found that the gain is somewhat lower, due to imperfect match, and is typically about 6 to 10 db for natural seismic events and about 8 to 10 db for the nuclear explosions.

Two examples of the application of matched filtering to long-period Rayleigh waves generated by nuclear explosions in the Eastern Kazakh area are shown in Figs. 13(a) and (b), along with the autocorrelation function of the reference waveform shown for $L = 600$ sec [Fig. 13(c)]. This result is quite typical for L in the range 500 to 800 sec, and is presented to illustrate the waveform which can be expected for a perfectly matched condition. The similarity of the autocorrelation function shown in Fig. 13 with the chirp-filtered trace shows that a relatively good match is obtained.

J. Capon
R. J. Greenfield

E. PATTERNS

The response patterns of LASA and other seismic arrays are usually computed and displayed as functions of relative wavenumber for sinusoidal signals. Although wavenumber is the natural argument of an array pattern mathematically, a display in wavenumber space is difficult to interpret in terms of the operational performance of an array beam. Moreover, seismic signals are wide-band transients, so that many of the details of the single-frequency patterns are irrelevant. In order to avoid these deficiencies, a study of wide-band array patterns has been carried out and a report which is in press[‡] will be briefly summarized here.

The output waveform from an array which is steered correctly, in speed and bearing, for a wide-band signal will be the same as that of the signal itself, but the output from an incorrectly steered array will be distorted. Thus, no single number can uniquely characterize the off-angle array response to a wide-band signal, and we have made the arbitrary choice of total energy (integral of the square of the array output waveform) as a suitable measure of wide-band array response. It then turns out that the array pattern so defined depends only on the signal power spectrum assumed, and we have derived a formula for the array response to a signal with a Gaussian spectrum. The center frequency and bandwidth of this spectrum are adjustable parameters, and the spectrum is symmetrized by the addition of an image Gaussian curve for negative

[†] J. R. Klauder, A. C. Price, S. Darlington, and W. J. Albersheim, "The Theory and Design of Chirp Radars," Bell System Tech. J. 39, 745 (1960).

[‡] E. J. Kelly, "Response of Seismic Arrays to Wide-Band Signals," Technical Note 1967-30, Lincoln Laboratory, M.I.T. (29 June 1967).

Section IV

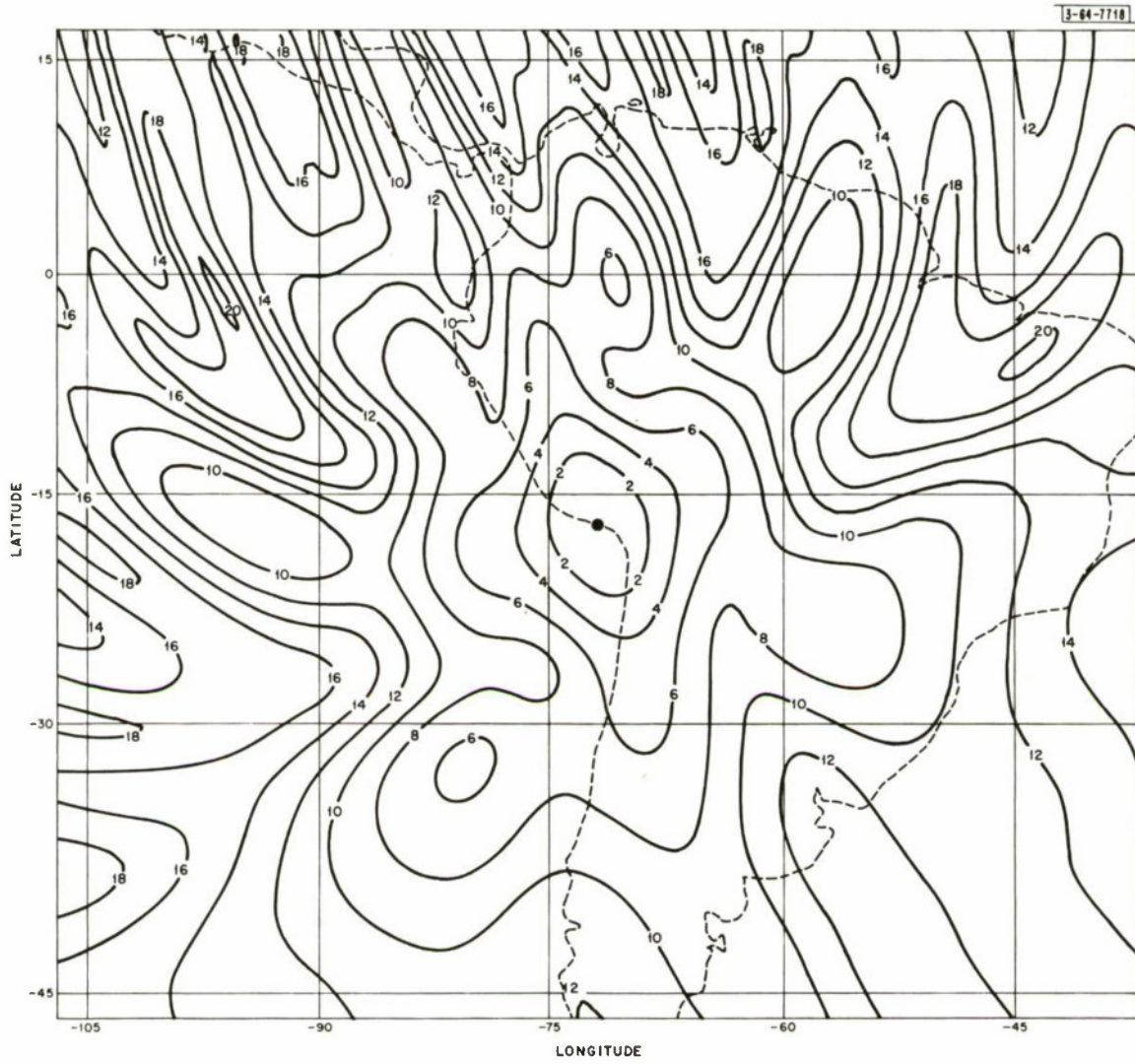


Fig. 14. LASA beam pattern for an epicenter in Peru.

frequencies. Patterns have been computed and contours plotted as functions of wavenumber (referred to the signal center frequency) for a variety of array geometries and signal bandwidths. The wide-band characteristic has a striking effect on the patterns, smearing out sidelobes and grating lobes and filling in nulls of the single-frequency patterns. In general, the patterns are considerably simpler for wide-band signals.

In order to see what the patterns for LASA (and several configurations made up of LASA subarrays) look like in real space, we took our results for a realistic signal model (center frequency 1 Hz, 3-db frequencies 0.76 and 1.24 Hz), picked various reference points in the earth, and contoured the patterns as functions of latitude and longitude in the vicinity of the reference point. As expected, the resulting contours are quite distorted in the transformation from wavenumber space to real space. An example is shown in Fig. 14, which is the pattern of the LASA array for a reference point on the coast of Peru.

The patterns just described are relevant to the operation of beamforming, where a variety of beams are formed to process an event at a fixed reference point. In the converse problem, the response of a fixed beam (steered at the reference point) to a variety of events at other points, it is necessary to correct the pattern for the variable effect of body-wave attenuation. This effect has been included and results in a further distortion of the patterns. In some cases, the difference in attenuation between events at the beam-steering point and off-angle is more than sufficient to offset the off-angle rejection factor of the normal pattern, resulting in "sidelobes" of larger response than the "main lobe." In Fig. 15, we show these effects for the LASA array, steered to the same reference point used in Fig. 14. The shaded region has response higher than the reference point, and the effect of core-boundary shadowing is clearly visible in the lower right corner.

E. J. Kelly

Section IV

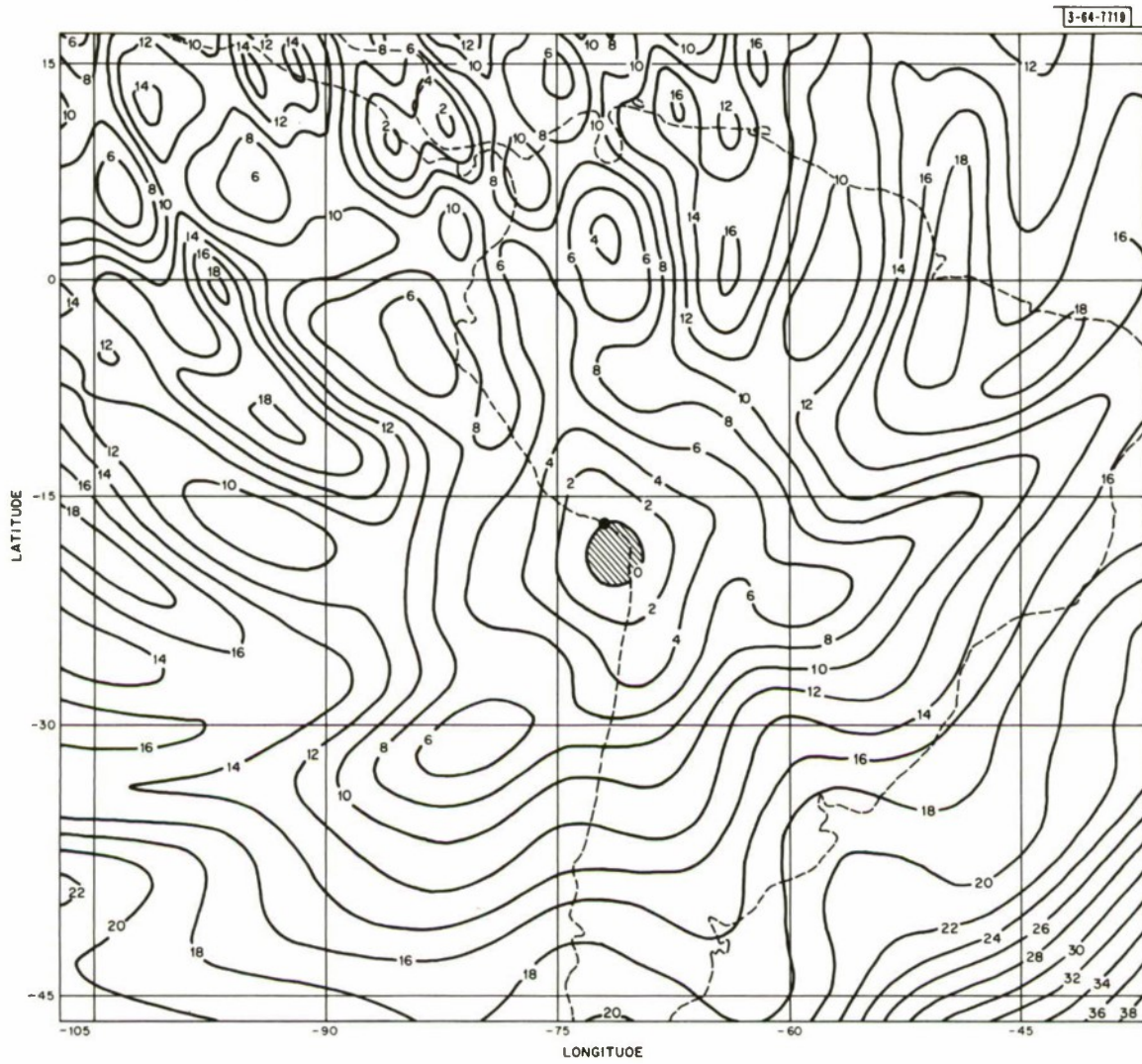


Fig. 15. LASA pattern, including attenuation, when array is steered to a point in Peru.

V. MONTANA LASA SYSTEM

A. AUTOMATIC MONITORING AND FAULT ANALYSIS

This system, referred to as the "Maintenance and Monitoring System," has been installed and is operating. For descriptions of the functions being performed see the previous SATSR (31 December 1966, DDC 646677).

Several minor changes in the previously described system have been made.

- (1) Statistical data, weather data, and communications with the operator are not being output on paper tape. Instead, a diagnostic program "PRINT" is available to the operator, allowing him to select, for printing on the console typewriter, any and/or all (stored) statistical data compiled by the system monitor.
- (2) An incremental magnetic-tape recorder was added to the system to allow the recording of selected data in special recording formats. At present, this recorder is collecting sensor and weather data in connection with the microbarograph experiment.
- (3) The proposed diagnostic program to perform a Fourier analysis of the 1-Hz sine-wave test signal was abandoned in view of the most encouraging results obtained from a similar analysis using the pseudo-random wideband calibration signal described earlier in the SATSR for 30 June 1966, Sec. VI (DDC 637308).

One function described in the previous report, that of intercommunication with the on-line PDP-7, is not yet operational. It is expected to be completed within a few weeks.

The monitor/fault diagnosis system is presently undergoing evaluation to determine the extent to which the previously assigned goals are being accomplished. The ability of the system to detect and identify component malfunctions and degradations as well as the usefulness of the diagnostic programs to further assist the Maintenance Supervisor in performing his duties has been demonstrated. It is too early to make conclusive statements concerning the overall effectiveness of the monitor/fault diagnosis experiment, although preliminary results indicate that the original goals will be achieved if not exceeded.

J. H. Helfrich
J. R. Brown
R. V. Wood, Jr.

B. LDC ANALOG SIGNAL DISTRIBUTION

A new analog signal distribution system has been installed at the LASA Data Center (LDC). This system now provides for a total of 96 input channels and 320 output channels. Input channel capacity could be expanded to 168 by the addition of appropriate smoothing filters.

In addition to providing a capability for patching any input to any output, the system provides weighting resistors for each output channel to provide calibration adjustment. Four 25-input summing amplifiers are provided, each designed so that its output is always correctly weighted as a function of the number of input signals applied.

Five basic timing signals are available: WWV, 1 Hz, LP time ticks, SP time ticks, and Vela code timing. Any of these timing signals may be connected to an output channel.

Calibration signals are provided, with controls which allow them to be switched into any output channels. A two-channel chart recorder is built into the distribution system and provides for visual observation of any two input or output channels.

Section V

Presently, outputs are being provided to 10 Develocorders, an FM telemetry system, and a 16-channel chart recorder.

Each separate Develocorder has its own calibration switching facility so that each channel may be individually calibrated without affecting any other recording.

A subarray simulator is provided, to permit a check of the entire system by providing digital inputs of selected patterns. This simulator may be connected in place of the Phone Line Interface System (PLINS), allowing total distribution system calibration and facilitating troubleshooting.

J. H. Helfrich
J. P. Densler

C. SUMMARY OF SYSTEM MODIFICATIONS AND TESTS PERFORMED BY PHILCO CORPORATION

During this reporting period, a large number of system measurements, modifications, and additions have been made to the array. Among the more important are the following.

1. Seismometer Environmental Measurements

Equipment has been designed and is under test for measuring the tilt angle of down-hole instruments under field conditions.

2. Alternate Seismometer Tests

A pair of shallow-hole Geotech seismometers (model 20171/25220) have been installed at site D2 and have performed satisfactorily for a number of months. Included with these seismometers are their associated solid-state amplifiers.

Initial field evaluation tests of the Mark Products L3A seismometer installed at B1-35 have been completed. In addition, bench tests on the Mandrel Industries EV-21V and the Geospace HS-10-1/B have been completed.

A combination HS-10-1/A and an RA-5 amplifier in an enlarged HS-10 case has been constructed, tested, and installed at site D2-46. A down-hole temperature probe has been co-located.

3. Standby Power Systems

Standby power systems have been constructed and installed at all 21 subarrays. An operating and maintenance manual has been prepared and a final report on the complete system is in preparation.

4. Ithaco Amplifiers

A field evaluation of the Ithaco model 154 seismic amplifiers has been completed.

5. Variometer Installation

Seven variometers were installed in the Montana LASA area, for three-component measurement of the earth's magnetic field by personnel of Southern Methodist University and of the Geology

and Geophysics Department at M.I.T. This work was sponsored by the Air Force Office of Scientific Research (AFOSR). Measurements were made over a period of five months, and the installation is now being dismantled.

6. Microbarograph Installation

An experimental microbarograph installation was made at site A0. Two systems, each consisting of the Pace model P90D transducer and a model CD10 modulator, were loaned from Hudson Laboratories.

Initial installation was made in the long-period Central Terminal Housing, and local chart recordings and remote transmission via the Subarray Electronics Module (SEM) were arranged. The second instrument was connected to a long pipe array filter.

Over a period of several months, evaluation has been completed on the two Pace systems, two Globe model 100-B systems, two Geotech systems, and one system from Karman Nuclear.

Laboratory tests at the LASA Maintenance Depot as well as field monitoring were performed on all systems. Reports are in preparation and will be available shortly.

The LP vaults at the B-ring sites have been modified to provide a controlled leak rate, and microbarograph systems are being installed there.

A second long pipe array is under construction at site A0 for further evaluation of the behavior of such filters.

7. Other Tasks

Numerous additional tasks, including both new installation and modifications, that were carried out during this period are: new weather station equipment, new seismometer amplifier power supplies, new calibration system for long-period seismometer, modification of long-period remote centering, modification of random pulse generators, and modifications of sub-array electronic modules.

R. V. Wood, Jr.
R. G. Enticknap

VI. SECOND LASA

To support the Defense Department's decision to build a second LASA as part of a continuing examination of the capabilities of large arrays, Lincoln Laboratory has suggested plans to ARPA for implementing such a program.

A. NORWEGIAN NOISE SURVEY

A plan, covering a noise survey of the selected area in Norway plus installation of a 21-sensor subarray, has been prepared. Figure 16 shows schematically the various elements in the plan.

The complete noise survey, to be effective in influencing future seismological work in the area, should provide data on the following items in order of importance:

- (1) Short-period noise level vs depth at one geographic location,
- (2) Long-period noise direction and velocity plus array gain vs sensor spacing at several geographic locations,
- (3) Short-period noise coherence vs sensor spacing at depth at one geographic location,
- (4) Short-period noise coherence vs sensor spacing at the surface at one geographic location in the array area,
- (5) Short-period noise level and spectra at several geographic locations in the proposed array area,
- (6) Long-period noise level and spectra at several points many tens of kilometers apart,
- (7) Short-period signal level at one geographic location,
- (8) Short-period signal coherence.

To answer these questions in a reasonable time, it is planned that a number of measurements be conducted in parallel. Some parameters can be roughly estimated from data already at hand; for example:

- (1) Using the Montana LASA, one can determine whether short-period noise correlation vs sensor spacing [item (3)] varies appreciably with sensor depth. An experiment to collect data for this measurement is now under way.
- (2) A small (7-element, 1-km spacing) short-period array now exists in Norway. Data from this small array, recorded on analog magnetic tape, are available and a number of reels have been analyzed. From these, one will be able to get partial data for items (1), (2), and (7) within the 3-km aperture of the small array.

It is clearly important that as much information as possible be extracted from the Montana LASA and from these existing magnetic tapes before the overseas measurements program begins, since the field program will be greatly influenced by these results.

For the presently existing Norway array, our estimate is that noise will be somewhat correlated across the 3-km aperture. Therefore, it is proposed to extend the two long legs of this array. The spacing of the two additional short-period sensors will be determined by our estimate of the noise correlation distance as determined from analysis of the analog magnetic tapes mentioned in paragraph (2) above. These two additional sensors will be surface installations.

Section VI

One wishes measurements of short-period noise at two locations, since it is expected that for this site, noise magnitude and coherence will be affected by proximity to the seacoast. Coincident with the measurements described in the previous paragraph, drilling will be started on two pairs of holes to the northwest of the present array. Drilling in this rock promises to be slow (perhaps 10 feet per day), so it is intended that the holes be drilled to about 200 feet and then cased.

In addition to the long-period, 3-component seismometer now installed at the present array, it is intended that three additional long-period instruments be installed as part of the noise survey.

At approximately the same time, work will start on the installation of a small array of short-period seismometers, probably to the north of the present array. This new array will have an aperture of 18 km and contain 21 seismometers approximately uniformly spaced within this aperture. At the time this array is installed, it is unlikely that useful data relating short-period noise statistics to sensor depth will be available. The present intent is to drill each short-period hole through the overburden and into the base rock about 40 feet before casing and cementing. To simplify the field work, one of the long-period survey stations will be made coincident with this short-period array. Signals from the 21 short-period sensors, plus long-period signals from one station, will be collected at a central point in the array for recording, probably by the digital recording van now being assembled at Lincoln Laboratory. The objective is to have the short-period array installed, with signals being recorded, by October 1967.

R. V. Wood, Jr. J. R. Brown
R. G. Enticknap R. M. Lerner
J. H. Helfrich

B. SEISMIC SYSTEM STUDIES

A tentative design for the entire array in Norway has been prepared and presented to ARPA.

1. Array Design Boundary Conditions

As presently seen, the principal considerations which affect array design are:

- (a) The short-period, on-line detection threshold should be equal to or greater than that achieved in Montana, that is, magnitude 3.5 at a 40° to 80° distance.
- (b) The long-period detection threshold must be at least as low as that observed in Montana, and hopefully lower.
- (c) Off-line, short-period processing by maximum likelihood will be needed only infrequently.
- (d) Off-line, long-period processing will take place on all events on which discrimination is to be performed and which are small enough to require it, and also on those events to be separated from interfering teleseisms.
- (e) Geometry must be adaptable to the host country land availability.
- (f) The array must operate with high reliability, giving continuity of surveillance.
- (g) Seismic data output to the host country seismologists should be at least as complete as that available to the United States.

- (h) "On-line" transmission to the United States should at most require a voice bandwidth circuit.
- (i) The array design must be economical and efficient, that is, capital and operating costs must be reasonably related to performance.

2. Array Description

The array configuration described here was arrived at by a study of the relationships among the relevant parameters. This configuration, which is proposed as an interim goal pending site survey data, is shown in Figs. 17 and 18. Particulars are as follows.

a. Short-Period Array Geometry

The short-period array consists of ten 20-sensor subarrays, equally spaced on the circumference of a 100-km circle. Subarray aperture is 18 km; within this aperture, sensors are distributed approximately uniformly, at a density of about 0.08 seismometer per km².

b. Long-Period Array Geometry

The long-period array consists of twenty 3-component sensors distributed over a 160-km aperture in such a way that the minimum spacing between sensors is about 30 km. Ten of these sensors are located in the short-period subarrays.

c. Short-Period On-Line Signal Processing

These processes include beamforming, event detection, and beam selection. Present indications are that these functions may be most efficiently and flexibly performed in a computing machine optimized for this purpose. This machine is labeled BED (beamformer-event detector) in Fig. 18. The interface couples the sensor data and control circuits to the BED as well as to the general-purpose computers. One of these computers controls the BED.

R. V. Wood, Jr. R. M. Lerner
R. G. Enticknap J. H. Helfrich

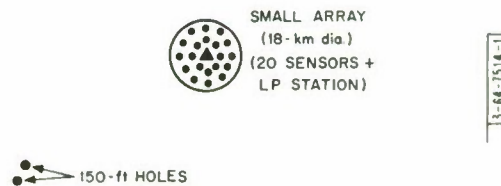


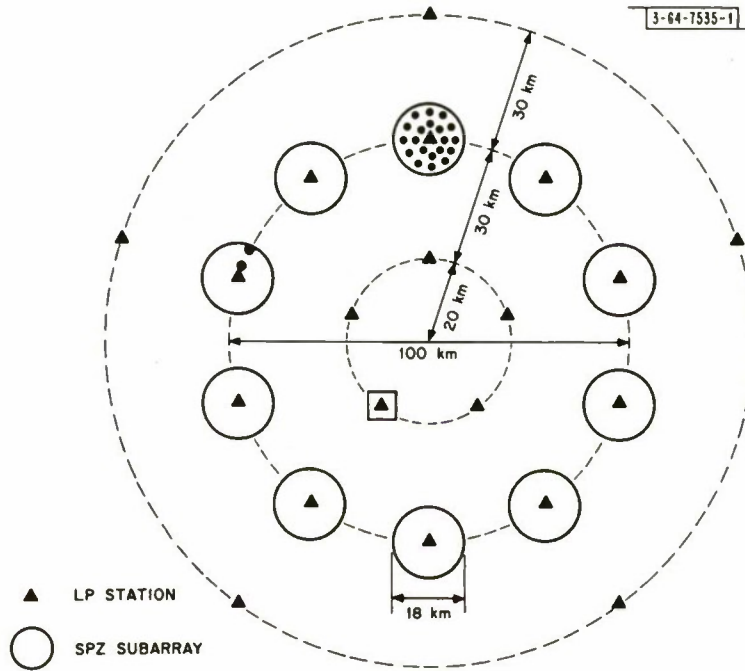
Fig. 16. Proposed noise survey station locations.

▲ PRESENT ARRAY (INCLUDING LP STATION)

▲ LP STATION

▲ LP STATION

Section VI



064-509

Fig. 17. Suggested layout of second large array. Site survey instrument locations from Fig. 16 are shown.

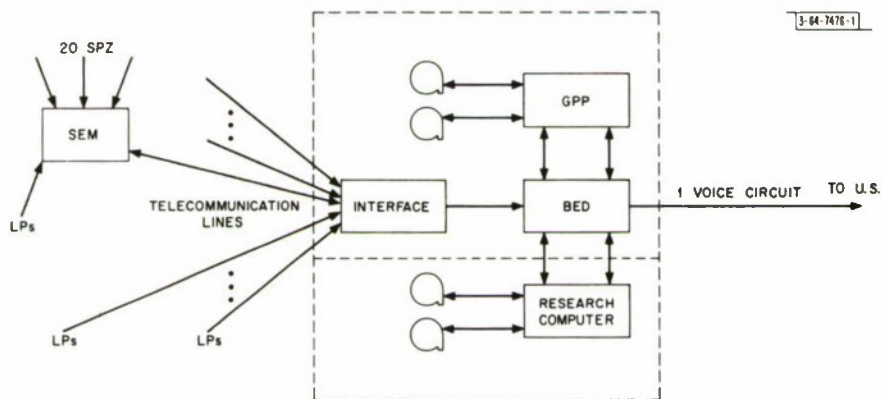


Fig. 18. Block diagram of second large array.

DOCUMENT CONTROL DATA - R&D

(Security classification of title, body of abstract and indexing annotation must be entered when the overall report is classified)

1. ORIGINATING ACTIVITY <i>(Corporate author)</i> Lincoln Laboratory, M.I.T.		2a. REPORT SECURITY CLASSIFICATION Unclassified	
		2b. GROUP None	
3. REPORT TITLE Semiannual Technical Summary Report to the Advanced Research Projects Agency on Seismic Discrimination			
4. DESCRIPTIVE NOTES <i>(Type of report and inclusive dates)</i> Semiannual Technical Summary Report - 1 January to 30 June 1967			
5. AUTHOR(S) <i>(Last name, first name, initial)</i> Green, Paul E.			
6. REPORT DATE 30 June 1967		7a. TOTAL NO. OF PAGES 44	7b. NO. OF REFS 14
8a. CONTRACT OR GRANT NO. AF 19 (628)-5167		9a. ORIGINATOR'S REPORT NUMBER(S) Semiannual Technical Summary (30 June 1967)	
b. PROJECT NO. ARPA Order 512		9b. OTHER REPORT NO(S) <i>(Any other numbers that may be assigned this report)</i> ESD-TR-67-325	
c.			
d.			
10. AVAILABILITY/LIMITATION NOTICES This document has been approved for public release and sale; its distribution is unlimited.			
11. SUPPLEMENTARY NOTES None		12. SPONSORING MILITARY ACTIVITY Advanced Research Projects Agency, Department of Defense	
13. ABSTRACT In continuation of work on networks embodying both large and small arrays, plans have been prepared for a second Large Aperture Seismic Array (LASA) station. Studies of on-line detection and location and also signal-to-noise improvement using large array structures are continuing. Significant progress in the discrimination area using relative excitation of body and surface waves is reported.			
14. KEY WORDS seismic array seismometers seismology			